

Aspects of Chirality Retention in Rearrangements of Pseudooctahedral Molybdenum and Tungsten Complexes

J. W. Faller,* D. A. Haitko, R. D. Adams,* and D. F. Chodosh

Contribution from the Department of Chemistry, Yale University,
New Haven, Connecticut 06520. Received July 21, 1978

Abstract: A mechanistic analysis of the rearrangements and structural investigation of a series of η^3 -allyl molybdenum and tungsten dicarbonyl bisphosphine complexes are presented. A three-dimensional crystallographic analysis revealed the structure of $(\eta^3\text{-C}_3\text{H}_5)\text{Mo}(\text{CO})_2(\text{diphos})\text{Cl}$ to be unlike that of the analogous diether and diamine chelates. Analysis of variable-temperature ^1H , ^{13}C , and ^{31}P NMR spectra have allowed the elucidation of the dynamic properties of these complexes. A trigonal twist rearrangement is proposed for the dynamic behavior of these complexes in which a rotation of the triangular face formed by the halogen and two phosphorus atoms relative to the face formed by the allyl and two carbonyl groups is involved. Barriers for this process are between 10 and 12 kcal/mol in the iodide derivatives. The twist process interconverts certain pairs of isomers while retaining particular elements of chirality, indicating that when complexes of this type rearrange a pathway for racemization may not necessarily be present.

Introduction

Isomeric structures of comparable thermodynamic stability are frequently found in organometallic systems. Many of these molecules may undergo rapid intramolecular rearrangements which interconvert the isomers and the processes can be detected by variations in the NMR spectra with temperature. These "stereochemically nonrigid"¹ structures include various coordination geometries;¹⁻⁴ however, in comparison with the well-known facile rearrangements of pentacoordinate complexes, relatively few fast intramolecular processes are known for six-coordinate species. This reflects the high stability of an octahedral arrangement of ligands relative to alternate hexacoordinate geometries, such as the trigonal prism. Of the reports which have appeared describing the dynamic stereochemistry of six-coordinate metal complexes the majority involve examinations of the twist rearrangements of a limited group of octahedral tris chelates whose barriers to interconversion are reported to range from 15 to 25 kcal/mol.⁵⁻⁷ While often found for tris chelate complexes, facile rearrangements would not, in general, be characteristic of hexacoordinate metal compounds. Most studies have involved isoleptic tris chelates and a given rearrangement process interconverts all of the possible isomers. One may be naively led to assume that if the molecule is nonrigid, all isomers would interconvert. This would lead to racemization in the case of optically active molecules. In view of the potential use of chiral metal complexes in asymmetric hydrogenations and asymmetric synthesis⁸⁻¹¹ we carried out an extensive investigation of a series of $(\eta^3\text{-C}_3\text{H}_5)\text{M}(\text{CO})_2(\text{P-P})\text{X}$ complexes, I-XV, where P-P is a bisphosphine ligand,¹² X is a halide, and M is either molybdenum or tungsten.

Four potentially stable configurations of these molecules are expected as shown in Figure 1. Crystal structure determinations of various diamine and diether analogues, $(\eta^3\text{-C}_3\text{H}_5)\text{Mo}(\text{CO})_2(\text{bpy})\text{NCS}$,¹³ $(\eta^3\text{-C}_3\text{H}_5)\text{Mo}(\text{CO})_2(\text{bpy})\text{-}(\text{py})^+\text{BF}_4^-$,¹⁴ $(\eta^3\text{-2-methylallyl})\text{Mo}(\text{CO})_2(\text{phen})\text{NCS}$,¹⁵ and $(\eta^3\text{-C}_3\text{H}_5)\text{Mo}(\text{CO})_2(\text{glyme})\text{OCOCF}_3$,¹⁶ indicate that the chelate together with the two carbonyl ligands form a horizontal plane while the trihapto ligand and the X group lie trans to one another in apical positions above and below the plane, A. Those molecules adopting configuration A (with symmetrical trihapto ligands) contain a plane of symmetry and therefore one would expect to observe equivalent carbonyl ligands in the low-temperature ^{13}C NMR spectra of these diamine and diether metal complexes. In contrast magnetic inequivalency of the carbonyl groups was observed in the low-temperature ^{13}C NMR spectra of the iodide complex, $(\eta^3\text{-}$

$\text{C}_3\text{H}_5)\text{W}(\text{CO})_2(\text{dppm})\text{I}$ (XII), suggesting that this compound had assumed configuration B, C, or D. Structure D was not consistent with the IR spectra. The correct structure from among the remaining possibilities was established by a three-dimensional X-ray crystallographic analysis of $(\eta^3\text{-C}_3\text{H}_5)\text{Mo}(\text{CO})_2(\text{diphos})\text{Cl}$ (I). Our preliminary work¹⁷ and recent publications¹⁸⁻²² indicated that complexes of this general type should exhibit unusual dynamic properties. Therefore, a detailed examination of the dynamic ^{31}P , ^1H , and ^{13}C NMR spectra of the complexes I-XV was carried out in order to discern the pathways and barriers to rearrangement for this series of pseudooctahedral metal complexes.

Results

Magnetic Resonance Studies. The ^1H NMR spectral data for the series of $(\eta^3\text{-allyl})\text{M}(\text{CO})_2(\text{P-P})\text{X}$ complexes I-XV are summarized in Table I and were obtained with ^{31}P decoupling to ensure accurate determination of coupling constants. Each of the complexes exhibits dynamic NMR spectra. Their room temperature $^1\text{H}\{^{31}\text{P}\}$ spectra exhibit three sets of resonances for the allyl moiety typical of the AA'BB'X spin system of symmetrical η^3 -allyl metal complexes. The ABCDX spin patterns observed in the limiting low-temperature ^1H spectra of the compounds demonstrate the magnetic non-equivalence of the methylene termini of the allyl ligand in the instantaneous structure. An intriguing feature of these spectra is the appearance of the methylene region of the coordinated bisphosphines. The methylene regions of complexes containing diphos (I,III,IV) appear as AA'BB' patterns in the averaged spectra. At -100°C , however, nonequivalence of each of the methylene protons of the diphos ligand is indicated by an ABCD pattern. An analysis of the AA'BB' spin system for these complexes was undertaken and the results are presented in Table II. Figure 2 shows the averaged ^1H NMR spectra of the methylene region of diphos in the complex $(\eta^3\text{-C}_3\text{H}_5)\text{Mo}(\text{CO})_2(\text{diphos})\text{Cl}$ (I), with and without phosphorus decoupling. A comparison with the methylene region of the diarsine ligand in $(\eta^3\text{-C}_3\text{H}_5)\text{Mo}(\text{CO})_2(\text{diars})\text{Cl}$ (XIII) is also made in Figure 2 illustrating the similarities to the phosphorus-decoupled spectrum of I.

In the dppm complexes IX-XII the methylene protons are inequivalent and exhibit a doublet of triplets pattern, each unequally split by phosphorus. The methylene protons display an AB pattern $\{^{31}\text{P}\}$ throughout the range of temperatures in which the allyl resonances average. The resonances of the vinyl protons in complexes containing the dppe group (V-VIII) were masked by the phenyl proton signals.

Table I. Proton Nuclear Magnetic Resonance Data

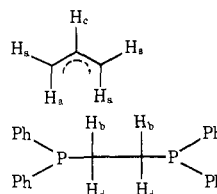
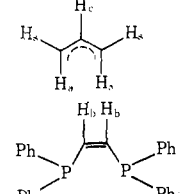
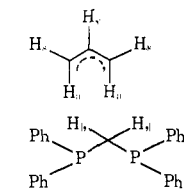
compd	assignment	δ^a	multiplicity ^b	intensity
I $(\eta^3\text{-C}_3\text{H}_5)\text{Mo}(\text{CO})_2(\text{diphos})\text{Cl}$ 	H _a	1.89	d ($J_{\text{H}_a\text{-H}_c} = 9.6$)	2
	H _s	3.66	m ($J_{\text{H}_s\text{-H}_c} = 5.7$) ($J_{\text{H}_s\text{-}^3\text{P}} = 2.8$)	2
	H _c	3.66	m	1
	H _b	2.95	m	2
	H _d	2.26	m	2
	phenyl	7.53	m	20
II $(\eta^3\text{-C}_3\text{H}_5)\text{Mo}(\text{CO})_2(\text{diphos})\text{I}$	H _a	1.82	d ($J_{\text{H}_a\text{-H}_c} = 9.7$)	2
	H _s	3.80	m ($J_{\text{H}_s\text{-H}_c} = 6.7$) ($J_{\text{H}_s\text{-}^3\text{P}} = 3.1$)	2
	H _c	4.05	m	1
	H _b	2.37	m	2
	H _d	3.14	m	2
	phenyl	7.40	m	20
III $(\eta^3\text{-C}_3\text{H}_5)\text{W}(\text{CO})_2(\text{diphos})\text{Cl}$	H _a	1.89	d of d ($J_{\text{H}_a\text{-H}_c} = 9.9$) ($J_{\text{H}_a\text{-}^3\text{P}} = 2.0$)	2
	H _s	3.43	m ($J_{\text{H}_s\text{-H}_c} = 6.6$) ($J_{\text{H}_s\text{-}^3\text{P}} = 3.2$)	2
	H _c	2.88	m	1
	H _b	2.98	m	2
	H _d	2.26	m	2
	phenyl	7.42	m	20
IV $(\eta^3\text{-C}_3\text{H}_5)\text{W}(\text{CO})_2(\text{diphos})\text{I}$	H _a	1.81	d ($J_{\text{H}_a\text{-H}_c} = 9.8$)	2
	H _s	3.64	m ($J_{\text{H}_s\text{-H}_c} = 6.5$) ($J_{\text{H}_s\text{-}^3\text{P}} = 3.0$)	2
	H _c	3.28	m	1
	H _b	3.17	m	2
	H _d	2.39	m	2
	phenyl	7.39	m	20
V $(\eta^3\text{-C}_3\text{H}_5)\text{Mo}(\text{CO})_2(\text{dppe})\text{Cl}$ 	H _a	1.94	d of d ($J_{\text{H}_a\text{-H}_c} = 10.1$) ($J_{\text{H}_a\text{-}^3\text{P}} = 2.0$)	2
	H _s	3.67	m ($J_{\text{H}_s\text{-H}_c} = 6.2$) ($J_{\text{H}_s\text{-}^3\text{P}} = 2.0$)	2
	H _c	3.75	m	1
	H _b	7.45	m	2
	phenyl	7.45	m	20
VI $(\eta^3\text{-C}_3\text{H}_5)\text{Mo}(\text{CO})_2(\text{dppe})\text{I}$	H _a	1.83	d ($J_{\text{H}_a\text{-H}_c} = 9.7$)	2
	H _s	3.81	m ($J_{\text{H}_c\text{-H}_s} = 6.7$) ($J_{\text{H}_s\text{-}^3\text{P}} = 3.4$)	2
	H _c	4.03	m	1
	H _b	7.43	m	2
	phenyl	7.43	m	20
VII $(\eta^3\text{-C}_3\text{H}_5)\text{W}(\text{CO})_2(\text{dppe})\text{Cl}$	H _a	1.87	d ($J_{\text{H}_a\text{-H}_c} = 10.0$)	2
	H _s	3.35	m ($J_{\text{H}_c\text{-H}_s} = 6.2$) ($J_{\text{H}_s\text{-}^3\text{P}} = 3.1$)	2
	H _c	2.99	m	1
	H _d	7.32	m	2
	phenyl	7.32	m	20
VIII $(\eta^3\text{-C}_3\text{H}_5)\text{W}(\text{CO})_3(\text{dppe})\text{I}$	H _a	1.86	d ($J_{\text{H}_a\text{-H}_c} = 9.5$)	2
	H _s	3.66	m ($J_{\text{H}_s\text{-H}_c} = 6.2$) ($J_{\text{H}_s\text{-}^3\text{P}} = 2.4$)	2
	H _c	3.36	m	1
	H _b	7.34	m	2
	phenyl	7.34	m	20
IX $(\eta^3\text{-C}_3\text{H}_5)\text{Mo}(\text{CO})_2(\text{dppm})\text{Cl}$ 	H _a	1.96	d ($J_{\text{H}_a\text{-H}_c} = 10.0$)	2
	H _s	3.77	m ($J_{\text{H}_s\text{-H}_c} = 6.4$) ($J_{\text{H}_s\text{-}^3\text{P}} = 3.6$)	2
	H _c	4.06	m	1
	H _b	4.46	m ($J_{\text{H}_b\text{-H}_d} = 13.9$) ($J_{\text{H}_b\text{-}^3\text{P}} = 11.2$)	1
	H _d	3.93	m ($J_{\text{H}_d\text{-H}_b} = 13.9$) ($J_{\text{H}_d\text{-}^3\text{P}} = 8.9$)	1
	phenyl	7.39	m	20

Table I (continued)

compd	assignment	δ^a	multiplicity ^b	intensity
X (η^3 -C ₃ H ₅)Mo(CO) ₂ (dppm)I	H _a	1.81	d ($J_{H_a-H_c} = 10.8$)	2
	H _s	3.77	m ($J_{H_s-H_c} = 6.5$) ($J_{H_s-^{31}P} = 2.8$)	2
	H _c	4.29	m	1
	H _b	4.19	m ($J_{H_b-H_d} = 14.5$) ($J_{H_b-^{31}P} = 8.8$)	1
	H _d	4.71	m ($J_{H_d-H_b} = 14.5$) ($J_{H_d-^{31}P} = 11.0$)	1
XI (η^3 -C ₃ H ₅)W(CO) ₂ (dppm)Cl	phenyl	7.30	m	20
	H _a	1.86	d ($J_{H_a-H_c} = 10.0$)	2
	H _s	3.42	m ($J_{H_s-H_c} = 7.5$) ($J_{H_s-^{31}P} = 2.7$)	2
	H _c	3.11	m	1
	H _b	4.38	m ($J_{H_b-H_d} = 15.0$) ($J_{H_b-^{31}P} = 12.3$)	1
XII (η^3 -C ₃ H ₅)W(CO) ₂ (dppm)I	phenyl	7.32	m	20
	H _a	1.86	d of d ($J_{H_a-H_c} = 10.3$) ($J_{H_a-^{31}P} = 1.5$)	2
	H _s	3.64	m ($J_{H_s-H_c} = 5.5$) ($J_{H_s-^{31}P} = 2.8$)	2
	H _c	3.55	m	1
	H _b	4.72	m ($J_{H_b-H_d} = 15.0$) ($J_{H_b-^{31}P} = 11.4$)	1
XIII (η^3 -C ₃ H ₅)Mo(CO) ₂ (diarsine)Cl	phenyl	7.38	m	20
	H _a	1.84	d ($J_{H_a-H_c} = 11.3$)	2
	H _s	3.66	d ($J_{H_s-H_c} = 6.3$)	2
	H _c	4.01	m	1
	H _b	2.84	m	2
XIV (η^3 -C ₃ H ₅)Mo(CO) ₂ (arphos)Cl	phenyl	7.41	m	20
	H _a	1.92	d ($J_{H_a-H_c} = 10.3$)	1
	H _{a'}	1.82	d of d ($J_{H_{a'}-H_c} = 10.3$) ($J_{H_{a'}-^{31}P} = 1.6$)	1
	H _s	3.73	m ($J_{H_s-H_c} = 7.7$) ($J_{H_s-H_{s'}} = 3.6$) ($J_{H_s-^{31}P} = <1.0$)	1
	H _{s'}	3.60	m ($J_{H_{s'}-H_c} = 7.7$) ($J_{H_{s'}-H_s} = 3.6$) ($J_{H_{s'}-^{31}P} = 5.4$)	1
XV (η^3 -C ₃ H ₅)Mo(CO) ₂ (arphos)I	H _c	3.85	m	1
	H _b	3.05	m	1
	H _d	2.78	m	1
	H _e	2.55	m	1
	H _f	2.01	m	1
	phenyl	7.39	m	20
	H _a	1.82	d ($J_{H_a-H_c} = 10.2$)	1
	H _{a'}	1.73	d of d ($J_{H_{a'}-H_c} = 10.2$) ($J_{H_{a'}-^{31}P} = 1.8$)	1
	H _s	3.86	m ($J_{H_s-H_c} = 6.8$) ($J_{H_s-H_{s'}} = 3.6$) ($J_{H_s-^{31}P} = <1.0$)	1
	H _{s'}	3.70	m ($J_{H_{s'}-H_c} = 6.8$) ($J_{H_{s'}-H_s} = 3.6$) ($J_{H_{s'}-^{31}P} = 6.8$)	1
H _c	4.12	m	1	
H _b	3.30	m	1	
H _d	2.91	m	1	
H _e	2.74	m	1	
H _f	2.05	m	1	
phenyl	7.39	m	20	

^a Chemical shifts are relative to Me₄Si as an internal standard and represent averaged spectra at 50 °C. Spectra were recorded in deuteriochloroform. ^b Splittings are given in hertz with s = singlet, d = doublet, t = triplet, d of d = doublet of doublets, and m = multiplet. Signs of the splittings were not determined.

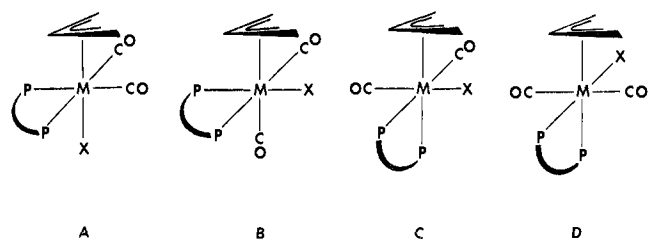


Figure 1. Possible structures for complexes of the general formula $(\eta^3\text{-C}_3\text{H}_5)\text{M}(\text{CO})_2(\text{P-P})\text{X}$.

Coupling of phosphorus to the syn and central protons of the allyl moiety was observed; however, in only two cases was coupling between phosphorus and the anti protons of the allyl group discerned. All of the protons contained in the bidentate phosphine ligands displayed splitting by phosphorus. Additional broadening is seen at low temperatures in the phenyl region presumably owing to restricted rotation about the phenyl carbon-phosphorus bonds. Further broadening is also seen in those complexes containing diphos which can be attributed to the $\lambda \rightleftharpoons \delta$ interconversion of chelate rings of diphos found to be rapid on the NMR time scale.

The ^{31}P NMR spectral data are summarized in Table III. For each compound a single resonance is observed in the room temperature spectrum; however, as one lowers the temperature this resonance broadens and then narrows into two (or four depending upon the resolution of ^{31}P - ^{31}P coupling) lines of equal intensity. Coupling of ^{183}W to phosphorus (on the order of 100 Hz) is observed in both the averaged and unaveraged spectra. The ^{13}C NMR data are summarized in Table IV. Couplings of ^{183}W to the carbon or proton nuclei were not observed.

In all cases, with the exception of the arphos derivative XIV, a single resonance is observed in the ^1H NMR room temperature spectra demonstrating the magnetic equivalence of the methylene termini of the allyl moiety at ambient temperature. For the diphos-containing complexes, I-IV, an apparent triplet

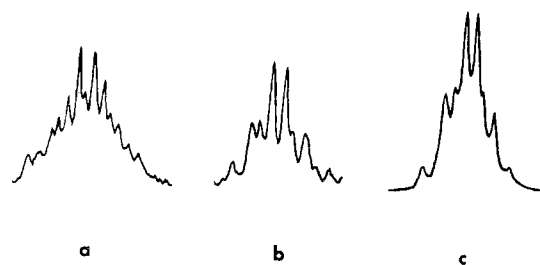


Figure 2. The ^1H NMR spectra illustrating the upfield half of the methylene region in $(\eta^3\text{-C}_3\text{H}_5)\text{Mo}(\text{CO})_2(\text{P-P})\text{Cl}$ complexes: (a) ^1H , P-P = diphos; (b) ^1H , ^{31}P , P-P = diphos; (c) ^1H , P-P = diars.

pattern is seen for the methylene protons at room temperature. The vinyl carbons (^{13}C NMR) of the complexes containing dppe, V-VIII, appear as a doublet of doublets at room temperature. The carbonyl carbons in the averaged spectrum appear as a multiplet. Coupling to phosphorus was observed for the carbonyl carbons, the methylene or vinyl carbons of the phosphine ligands, as well as the phenyl carbons, but not to the allylic carbons. At low temperature the carbonyl carbons, terminal carbons of the allyl, methylene, or vinyl carbon resonances each broaden and then sharpen into two (or more resonances depending upon the resolution of ^{31}P - ^{13}C coupling) resonances of equal intensity. The carbonyl carbons show unequal coupling to phosphorus at low temperatures.

All complexes showed carbonyl bands at approximately 1940 and 1840 cm^{-1} . Owing to insolubility in cyclohexane the spectra were recorded in methylene chloride solution, and therefore exhibit broad bands with half-widths of ~ 20 cm^{-1} . The intensities of the two carbonyl absorptions were approximately equal, characteristic of cis coordinated carbonyl ligands.

Description of the Structure of I. The molecular structure of $(\eta^3\text{-C}_3\text{H}_5)\text{Mo}(\text{CO})_2(\text{diphos})\text{Cl}$ is shown in Figure 3, and pertinent crystallographic parameters are given in Tables V-VIII. The molecule can be conveniently described as pseudooctahedral with the assumption that the allyl moiety

Table II. Coupling Constants of the Methylene Region of Diphos in the Complexes $(\eta^3\text{-C}_3\text{H}_5)\text{M}(\text{CO})_2(\text{diphos})\text{X}$

compd	N^a		$(M^2 + L^2)^{1/2}$ a		calcd coupling constants		
	calcd	obsd	calcd	obsd	J_{AB}	$J_{AB'}$	$J_{AA'}$
I $(\eta^3\text{-C}_3\text{H}_5)\text{Mo}(\text{CO})_2(\text{diphos})\text{Cl}$	5.5	5.5	22.5	2.6	-14.0	+8.5	+5.5
XIII $(\eta^3\text{-C}_3\text{H}_5)\text{Mo}(\text{CO})_2(\text{diarsine})\text{Cl}$	4.4	4.4	21.6	21.3	-13.1	+8.7	+5.9
III $(\eta^3\text{-C}_3\text{H}_5)\text{W}(\text{CO})_2(\text{diphos})\text{Cl}$	6.1	6.1	23.5	23.3	-14.8	+9.1	+5.5
IV $(\eta^3\text{-C}_3\text{H}_5)\text{W}(\text{CO})_2(\text{diphos})\text{I}$	6.1	6.1	22.7	22.4	-14.4	+8.5	+6.3

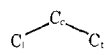
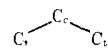
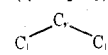
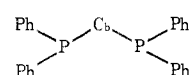
a The separations are based upon the following relationships: $K = J_{AA'} + J_{BB'}$; $M = J_{AA'} - J_{BB'}$; $\nu_1 - \nu_3 = N$; $L = J_{AB} - J_{AB'}$; $N = J_{AB} + J_{AB'}$; $(M^2 + L^2)^{1/2} = \nu_9 - \nu_{11}$. The signs of J are based upon the following observations: $J_{AB} = (-)$ for geminal protons of disubstituted ethane; $J_{AB'} = (+)$ for vicinal trans protons of disubstituted ethane; $J_{AA'} = (+)$ for vicinal gauche protons of disubstituted ethane.

Table III. ^{31}P Nuclear Magnetic Resonance Data

compd	temp, K	solvent	δ^a	$ J_{^{183}\text{W } ^{31}\text{P}} $
$(\eta^3\text{-C}_3\text{H}_5)\text{Mo}(\text{CO})_2(\text{diphos})\text{Cl}$	307.5	CDCl_3	44.04	
$(\eta^3\text{-C}_3\text{H}_5)\text{Mo}(\text{CO})_2(\text{diphos})\text{I}$	256	CD_2Cl_2	38.73	
$(\eta^3\text{-C}_3\text{H}_5)\text{Mo}(\text{CO})_2(\text{arphos})\text{I}$	298	$\text{CH}_2\text{Cl}_2/\text{PhCD}_3$	42.91	
$(\eta^3\text{-C}_3\text{H}_5)\text{W}(\text{CO})_2(\text{diphos})\text{Cl}$	307.5	CDCl_3	31.02	98.7
$(\eta^3\text{-C}_3\text{H}_5)\text{W}(\text{CO})_2(\text{diphos})\text{I}$	298	$\text{CH}_2\text{Cl}_2/\text{PhCD}_3$	22.59	97.9
$(\eta^3\text{-C}_3\text{H}_5)\text{Mo}(\text{CO})_2(\text{dppe})\text{Cl}$	307.5	CDCl_3	53.21	
$(\eta^3\text{-C}_3\text{H}_5)\text{Mo}(\text{CO})_2(\text{dppe})\text{I}$	298	$\text{CH}_2\text{Cl}_2/\text{PhCD}_3$	45.65	
$(\eta^3\text{-C}_3\text{H}_5)\text{W}(\text{CO})_2(\text{dppe})\text{Cl}$	307.5	$\text{CH}_2\text{Cl}_2/\text{PhCD}_3$	42.07	96.2
$(\eta^3\text{-C}_3\text{H}_5)\text{W}(\text{CO})_2(\text{dppe})\text{I}$	307	$\text{CH}_2\text{Cl}_2/\text{C}_2\text{D}_6\text{CO}$	29.42	100.1
$(\eta^3\text{-C}_3\text{H}_5)\text{Mo}(\text{CO})_2(\text{dppm})\text{Cl}$	307.5	CDCl_3	-2.01	
$(\eta^3\text{-C}_3\text{H}_5)\text{Mo}(\text{CO})_2(\text{dppm})\text{I}$	286	CD_2Cl_2	-11.01	
$(\eta^3\text{-C}_3\text{H}_5)\text{W}(\text{CO})_2(\text{dppm})\text{Cl}$	307.5	CDCl_3	-19.52	93.3
$(\eta^3\text{-C}_3\text{H}_5)\text{W}(\text{CO})_2(\text{dppm})\text{I}$	300	$\text{CH}_2\text{Cl}_2/\text{CD}_2\text{Cl}_2$	-25.11	b

a All shifts referenced to H_3PO_4 and CDCl_3 deuterium lock. b ^{183}W - ^{31}P satellites not resolved at this temperature owing to broad resonance.

Table IV. Room Temperature Carbon-13 Nuclear Magnetic Resonance Data

compd	assignment	δ^a	$J(^{31}\text{P}-^{13}\text{C})^b$
I $(\eta^3\text{-C}_3\text{H}_5)\text{Mo}(\text{CO})_2(\text{diphos})\text{Cl}$ 	C_t	60.42	n.r.
	C_c	83.69	n.r.
	C_b	25.82	18.9
	phenyl	130.25	complex
	CO	244.03	n.r.
II $(\eta^3\text{-C}_3\text{H}_5)\text{Mo}(\text{CO})_2(\text{diphos})\text{I}$	C_t	57.80	n.r.
	C_c	77.10	n.r.
	C_b	26.83	22.0
	phenyl	130.16	complex
	CO	223.14	n.r.
III $(\eta^3\text{-C}_3\text{H}_5)\text{W}(\text{CO})_2(\text{diphos})\text{Cl}$	C_t	52.40	n.r.
	C_c	73.75	n.r.
	C_b	26.57	complex
	phenyl	130.45	complex
	CO	214.74	n.r.
IV $(\eta^3\text{-C}_3\text{H}_5)\text{W}(\text{CO})_2(\text{diphos})\text{I}$	C_t	49.74	n.r.
	C_c	71.12	n.r.
	C_b	27.20	30.3
	phenyl	130.31	complex
V $(\eta^3\text{-C}_3\text{H}_5)\text{Mo}(\text{CO})_2(\text{dppe})\text{Cl}$ 	CO	213.19	8.4
	C_t	60.39	n.r.
	C_c	82.94	n.r.
	C_b	144.72	34.9
	phenyl	133.40	complex
VI $(\eta^3\text{-C}_3\text{H}_5)\text{Mo}(\text{CO})_2(\text{dppe})\text{I}$	CO	223.26	10.8
	C_t	57.68	n.r.
	C_c	79.80	n.r.
	C_b	146.16	27.0
	phenyl	130.75	complex
VII $(\eta^3\text{-C}_3\text{H}_5)\text{W}(\text{CO})_2(\text{dppe})\text{Cl}$	CO	223.13	9.0
	C_t	52.21	n.r.
	C_c	73.01	n.r.
	C_b	143.33	31.5
	phenyl	130.64	complex
VIII $(\eta^3\text{-C}_3\text{H}_5)\text{W}(\text{CO})_2(\text{dppe})\text{I}$	CO	216.14	n.r.
	C_t	49.58	n.r.
	C_c	71.16	n.r.
	C_b	147.16	31.8
	phenyl	130.58	complex
IX $(\eta^3\text{-C}_3\text{H}_5)\text{Mo}(\text{CO})_2(\text{dppm})\text{Cl}$ 	CO	212.76	n.r.
	C_t	59.94	n.r.
	C_c	85.23	n.r.
	C_b	36.21	19.5
	phenyl	130.36	complex
X $(\eta^3\text{-C}_3\text{H}_5)\text{Mo}(\text{CO})_2(\text{dppm})\text{I}$ 	CO	225.46	8.3
	C_t	56.65	n.r.
	C_c	81.63	n.r.
	C_b	36.52	22.0
	phenyl	130.05	complex
XII $(\eta^3\text{-C}_3\text{H}_5)\text{W}(\text{CO})_2(\text{dppm})\text{I}$	CO	224.79	10.7
	C_t	48.48	n.r.
	C_c	72.57	n.r.
	C_b	38.05	25.3
	phenyl	130.46	comple:
XV $(\eta^3\text{-C}_3\text{H}_5)\text{Mo}(\text{CO})_2(\text{arphos})\text{I}$	CO	214.95	n.r.
	C_t (1)	57.33	n.r.
	C_t (2)	55.92	n.r.
	C_c	77.89	n.r.
	As- CH_2	23.49	6.9
	P- CH_2	28.07	14.9
	CO(1)	189.53	8.7
	CO(2)	191.52	10.7
phenyl	130.55	complex	

^a Chemical shifts are relative to Me₄Si in CDCl₃ solutions with 0.5 M Cr(acac)₃ used as a relaxation reagent. The spectra were recorded at -23 °C. ^b Splittings are given in hertz unless not resolved. No ¹⁸³W-¹³C splittings were observed.

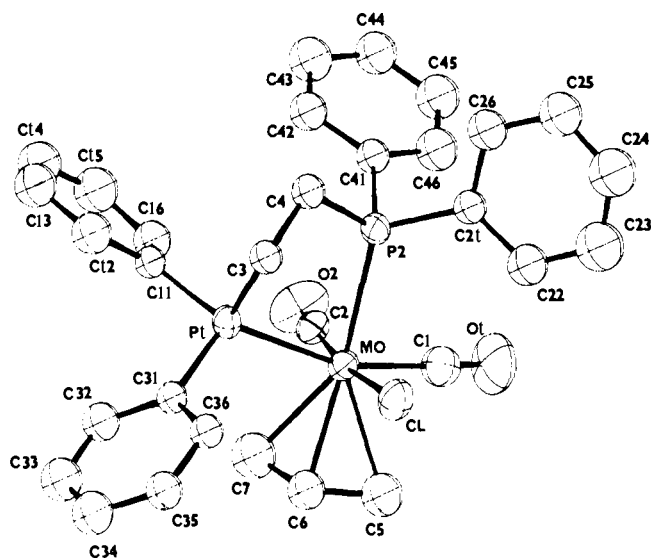


Figure 3. A perspective view of $(\eta^3\text{-C}_3\text{H}_5)\text{Mo}(\text{CO})_2(\text{diphos})\text{Cl}$. Hydrogen atoms are not shown.

occupies one coordination site. The molybdenum atom is surrounded by six ligands including an allyl group, two terminally coordinated carbonyl groups, the bidentate diphos ligand, and a chlorine atom. An equatorial plane (see Table VIII) can be defined to include the two carbonyls (C1-O1, C2-O2), the halogen (Cl), and one of the phosphorus atoms (P1) of the diphos ligand. The $\eta^3\text{-C}_3\text{H}_5$ group and the second phosphorus atom of the chelate (P2) lie trans to one another occupying the so-called apical positions in the pseudooctahedral coordination geometry. Final atomic coordinates are listed in Table V. Pertinent bond distances and angles are given in Tables VI and VII, respectively. The description and equations for various unit weighted least-squares molecular planes and distances of selected atoms to these planes are given in Table VIII.

The angle subtended at the molybdenum atom by the two phosphorus atoms of the diphos is $75.3 (1)^\circ$. This causes some distortion from an ideal octahedral arrangement. A comparison to other molybdenum complexes containing diphos ligands shows that a small P-Mo-P angle is common, viz., $75.3 (1)^\circ$ for $(\eta^5\text{-C}_5\text{H}_5)\text{Mo}(\text{diphos})(\text{CO})\text{Cl}$,²³ $76.5 (1)^\circ$ for $\text{Mo}(\text{CO})_3(\text{diphos})\text{Br}_2\text{-acetone}$,²⁴ and $79.7 (3)^\circ$ for $(\text{SnCl}_3)\text{Mo}(\text{CO})_4(\text{diphos})$.²⁵ The "bite" or P...P distance is $2.94 (5) \text{ \AA}$, which is somewhat smaller than the P...P distance for $(\text{diphos})\text{Mo}(\text{CO})_3(\text{Br})_2\text{-acetone}$ (3.17 \AA) and the 3.29 \AA distance reported for the compound $(\text{SnCl}_3)\text{Mo}(\text{CO})_4(\text{diphos})$. The molybdenum-phosphorus bond lengths, Mo-P1 = $2.592 (3) \text{ \AA}$ and Mo-P2 = $2.529 (4) \text{ \AA}$, appear to be normal. The molybdenum-chlorine distance, Mo-Cl = $2.573 (4) \text{ \AA}$, agrees favorably with the reported values of $2.452 (9)$ and $2.541 (5) \text{ \AA}$ for the compounds $(\eta^5\text{-C}_5\text{H}_5)\text{Mo}(\text{CO})_3\text{Cl}$ ¹⁵ and $(\eta^5\text{-C}_5\text{H}_5)\text{Mo}(\text{CO})(\text{diphos})\text{Cl}$, respectively.

The carbonyl ligands are essentially linear with Mo-C7-O1 = $173 (1)^\circ$ and Mo-C2-O2 = $176 (1)^\circ$. The values for the molybdenum-carbonyl angles are similar to those found for other terminal carbonyls contained in molybdenum systems. The Mo-CO and C-O distances are both within the range of values reported for other molybdenum carbonyl complexes.²³⁻²⁷

The allyl group has an intercarbon angle of $116 (1)^\circ$, which is consistent with the values of $115.7 (1)^\circ$ for $(\eta^3\text{-C}_3\text{H}_5)\text{Mo}(\text{CO})_2(\text{bpy})(\text{NCS})$,¹³ $111.5 (2)^\circ$ for $(\eta^3\text{-2-methylallyl})\text{Mo}(\text{CO})_2(\text{phen})(\text{NCS})$,¹⁵ $111.4 (1)^\circ$ for $(\eta^3\text{-C}_3\text{H}_5)\text{Mo}(\text{CO})_2(\text{bpy})\text{py}^+\text{BF}_4^-$,¹⁴ and $117 (2)^\circ$ for $(\text{Et}_2\text{Bpz}_2)(\eta^3\text{-C}_3\text{H}_5)\text{Mo}(\text{CO})_2$.²⁷ The mean C-C bond length of $1.397 (17) \text{ \AA}$ is in good agreement with the values reported for nu-

Table V. Atomic Coordinates for $(\eta^3\text{-C}_3\text{H}_5)\text{Mo}(\text{CO})_2(\text{diphos})\text{Cl}$

atom	X/a	Y/b	Z/c
Mo	0.218 60 (12)	0.076 30 (6)	0.202 01 (7)
Cl	0.409 63 (33)	0.026 06 (17)	0.327 26 (19)
P1	0.214 22 (32)	0.159 71 (17)	0.346 65 (19)
P2	0.360 04 (33)	0.183 13 (17)	0.196 14 (19)
O1	0.2628 (11)	0.0189 (6)	0.0126 (6)
C1	0.2525 (14)	0.0372 (7)	0.0857 (8)
O2	0.0158 (10)	0.1446 (5)	0.0362 (6)
C2	0.0891 (13)	0.1215 (6)	0.0991 (8)
C11	0.1154 (11)	0.2421 (6)	0.3289 (7)
C12	0.1232 (14)	0.2902 (7)	0.4060 (8)
C13	0.0537 (14)	0.3543 (7)	0.3930(9)
C14	0.9819 (14)	0.3713 (7)	0.3039 (9)
C15	0.9744 (15)	0.3264 (7)	0.2277 (9)
C16	0.0404 (13)	0.2606 (7)	0.2395 (7)
C21	0.5109 (12)	0.1647 (6)	0.1817 (7)
C22	0.5505 (14)	0.0922 (7)	0.1702 (8)
C23	0.6645 (16)	0.0801 (9)	0.1573 (9)
C24	0.7345 (17)	0.1396 (8)	0.1554 (9)
C25	0.7021 (15)	0.2107 (8)	0.1639 (9)
C26	0.5874 (14)	0.2255 (7)	0.1764 (8)
C3	0.3671 (12)	0.2151 (6)	0.3892 (7)
C4	0.3946 (12)	0.2420 (6)	0.3069 (7)
C31	0.1857 (11)	0.1151 (6)	0.4523 (7)
C32	0.0745 (13)	0.1221 (7)	0.4707 (8)
C33	0.5556 (14)	0.4123 (7)	0.0505 (8)
C34	0.6451 (15)	0.4532 (7)	0.1102 (9)
C35	0.7564 (13)	0.4621 (7)	0.0934 (8)
C36	0.7808 (11)	0.4277 (9)	0.0137 (7)
C41	0.3017 (12)	0.2474 (6)	0.0960 (7)
C42	0.2352 (13)	0.3117 (7)	0.1009 (7)
C43	0.1905 (15)	0.3558 (7)	0.0202 (9)
C44	0.7096 (14)	0.1646 (7)	0.4344 (8)
C45	0.7701 (15)	0.2267 (8)	0.4271 (9)
C46	0.3161 (14)	0.2280 (7)	0.0076 (8)
C5	0.3269 (14)	0.4494 (7)	0.3141 (8)
C6	0.3717 (13)	0.4833 (6)	0.2444 (8)
C7	0.0325 (15)	0.0333 (7)	0.2208 (9)

Table VI. Bond Distances for $(\eta^3\text{-C}_3\text{H}_5)\text{Mo}(\text{CO})_2(\text{diphos})\text{Cl}$

atoms	distance, \AA	atoms	distance, \AA
Mo-Cl	2.573 (4)	C14-C15	1.352 (5)
Mo-P1	2.592 (3)	C15-C16	1.387 (17)
Mo-P2	2.529 (4)	C21-C22	1.406 (16)
Mo-C1	1.966 (13)	C22-C23	1.385 (23)
Mo-C2	1.955 (13)	C23-C24	1.341 (21)
Mo-C5	2.340 (12)	C24-C25	1.348 (18)
Mo-C6	2.221 (12)	C25-C26	1.399 (22)
Mo-C7	2.350 (17)	C31-C32	1.376 (19)
C1-O1	1.147 (13)	C32-C33	1.383 (15)
C2-O2	1.127 (14)	C33-C34	1.354 (18)
P1-C11	1.837 (11)	C34-C35	1.370 (22)
P1-C31	1.839 (11)	C35-C36	1.407 (15)
P1-C3	1.839 (13)	C41-C42	1.397 (16)
P2-C21	1.824 (13)	C42-C43	1.386 (15)
P2-C41	1.829 (11)	C43-C44	1.374 (16)
P2-C4	1.871 (10)	C44-C45	1.334 (17)
C3-C4	1.507 (14)	C45-C46	1.397 (15)
C11-C12	1.397 (14)	C5-C6	1.397 (17)
C12-C13	1.383 (17)	C6-C7	1.397 (18)
C13-C14	1.354 (16)		

merous molybdenum-allylic systems. There are no structural features in the complex which indicate unusual deviations or distortions.

Discussion

The low-temperature ^{13}C NMR spectrum of $(\eta^3\text{-C}_3\text{H}_5)\text{W}(\text{CO})_2(\text{dppm})\text{I}$ (XII) is shown in Figure 4 (expanded carbonyl region). The ^{31}P coupling to each of two carbonyl reso-

Table VII. Bond Angles for (η^3 -C₃H₅)Mo(CO)₂(diphos)Cl

atoms	angle, deg	atoms	angle, deg
Mo-Cl-O1	173 (1)	P1-C11-C16	121.4 (9)
Mo-C2-O2	176 (1)	P1-C31-C32	121 (1)
C1-Mo-C2	77.6 (5)	P1-C31-C36	118 (1)
C1-Mo-C ℓ	98.4 (4)	C11-P1-C31	102.8 (5)
C2-Mo-C ℓ	172.1 (4)	C3-P1-C11	101.8 (5)
P1-Mo-P2	75.3 (1)	C3-P1-C31	106.0 (5)
P1-Mo-C ℓ	80.8 (1)	Mo-P2-C21	120.0 (4)
P2-Mo-C ℓ	82.5 (1)	Mo-P2-C41	114.6 (4)
P1-Mo-C1	163.0 (4)	P2-C21-C22	122 (1)
P1-Mo-C2	101.1 (3)	P2-C21-C26	119 (1)
P2-Mo-C1	87.7 (4)	P2-C41-C42	124.3 (9)
P2-Mo-C2	90.5 (4)	P2-C41-C46	118 (1)
Mo-C6-C7	77.3 (8)	C21-P2-C41	99.6 (6)
Mo-C6-C5	76.9 (8)	C4-P2-C21	103.1 (5)
C5-C6-C7	116 (1)	C4-P2-C41	105.3 (5)
C6-Mo-P2	161.9 (3)	C11-C12-C13	120 (1)
C6-Mo-P1	92.0 (3)	C12-C13-C14	119 (1)
C6-Mo-C1	105.9 (4)	C13-C14-C15	122 (1)
C6-Mo-C2	112.5 (4)	C14-C15-C16	120 (1)
C6-Mo-C ℓ	82.7 (3)	C15-C16-C11	120 (1)
Mo-P1-C3	105.9 (4)	C16-C11-C12	119 (1)
Mo-P2-C4	112.5 (4)	C21-C22-C23	121 (2)
P2-C4-C3	111.4 (1)	C22-C23-C24	118 (2)
P1-C3-C4	108.9 (8)	C23-C24-C25	125 (2)
Mo-P1-C11	120.5 (3)	C24-C25-C26	119 (2)
Mo-P1-C31	188.0 (4)	C25-C26-C21	118 (1)
P1-C11-C12	119.5 (9)	C26-C21-C22	119 (1)
C5-Mo-C ℓ	81.2 (3)	C7-Mo-C2	73.3 (5)
C5-Mo-C7	60.5 (5)	C7-Mo-P1	82.5 (3)
C5-Mo-P1	126.3 (3)	C7-Mo-P2	149.5 (3)
C5-Mo-P2	149.9 (4)	C7-Mo-C ℓ	114.6 (3)
C5-Mo-C ℓ	69.9 (5)	C7-Mo-Cl	112.8 (5)
C31-C32-C33	120 (1)		
C32-C33-C34	121 (2)		
C33-C34-C35	121 (1)		
C34-C35-C36	120 (1)		
C35-C36-C31	117 (1)		
C36-C31-C32	121 (1)		
C41-C42-C43	120 (1)		
C42-C43-C44	120 (1)		
C43-C44-C45	121 (1)		
C44-C45-C46	120 (1)		
C45-C46-C41	121 (1)		
C46-C41-C42	118 (2)		

nances is quite well resolved at -90°C . The ^{31}P - ^{13}C coupling of these resonances is a key feature in determining the relative positions of phosphorus atoms and carbonyl ligands. The ^{31}P - ^{13}C couplings of the analogous complexes $\text{M}(\text{CO})_4(\text{diphos})$ where $\text{M} = \text{Mo}, \text{W}$ have been studied by Randall et al.²⁸ It was reported that the carbonyls trans to phosphorus exhibited a larger ^{31}P - ^{13}C coupling than those oriented cis to phosphorus; the trans ^{31}P - ^{13}C coupling was reported as two to three times larger than cis coupling. Examination of the carbonyl region in Figure 4 shows that the carbonyl carbon at 214.16 ppm shows a substantially greater and more complex splitting by phosphorus than the carbonyl carbon at 215.82 ppm. The coupling pattern indicates that the carbonyl carbon at 214.16 ppm exhibits both cis and trans coupling to phosphorus whereas the carbonyl carbon at lower field exhibits only cis ^{31}P - ^{13}C coupling. Both structures B and C (Figure 1) are consistent with this coupling pattern; however, in structure A each carbonyl should show cis and trans ^{31}P - ^{13}C coupling. Structure D is inconsistent with the observation of two nearly equally intense carbonyl absorption bands in the IR. The molecular configuration was conclusively determined by a three-dimensional X-ray crystallographic analysis. Since all of the complexes of the general formula $(\eta^3\text{-C}_3\text{H}_5)\text{M}(\text{CO})_2(\text{P-P})\text{X}$ have similar NMR and infrared spectra, one

Table VIII. Various Unweighted Least-Squares Planes for $(\eta^3\text{-C}_3\text{H}_5)\text{Mo}(\text{CO})_2((\text{C}_6\text{H}_5)_2\text{P}(\text{CH}_2)_2\text{P}(\text{C}_6\text{H}_5)_2)\text{Cl}$

plane	atoms	distance from plane, Å
	C11	0.0048
	C12	-0.0145
1	C13	0.0126
	C14	-0.0007
	C15	-0.0090
	C16	0.0068
	C21	0.0146
	C22	-0.0069
2	C23	-0.0045
	C24	0.0079
	C25	0.0006
	C25	-0.0116
	C31	0.0030
	C32	-0.0045
3	C33	0.0011
	C34	0.0038
	C35	-0.0052
	C36	0.0018
	C41	0.0160
	C42	-0.0111
4	C43	-0.0006
	C44	0.0077
	C45	-0.0025
	C46	-0.0095
	C5	0.0
5	C6	0.0
	C7	0.0
	Mo*	2.0174
	Cl	0.0791
	P1	-0.0768
6	C1	-0.1077
	C2	0.1054
	Mo ^a	0.2365

planes	dihedral angle, deg
1-2	83.1
1-3	116.6
2-3	58.5
1-4	155.2
2-4	72.6
3-4	45.5
1-5	155.8
2-5	83.2
3-5	39.4
4-5	18.0
1-6	17.1
2-6	82.6
3-6	128.3
4-6	152.5
5-6	165.6

Equation for Planes Are of the Form $Ax + By + Cz - D = 0$

plane	A	B	C	D
1	-9.673	-8.819	6.257	-1.197
2	1.358	-0.995	12.723	2.828
3	2.102	14.456	6.797	5.125
4	9.388	9.321	-0.227	5.101
5	7.583	13.380	-1.633	0.332
6	-7.611	-13.037	5.123	-1.860

can assume that their molecular structure is analogous to that of $(\eta^3\text{-C}_3\text{H}_5)\text{Mo}(\text{CO})_2(\text{diphos})\text{Cl}$. The molecular structure is like that of configuration C (Figure 1) and is unlike that of the analogous diamine or diether complexes (vide supra), which have structure A.¹³⁻¹⁵

Mechanism of Interconversion. The barriers to rearrangement for these complexes are approximately 11 kcal/mol and

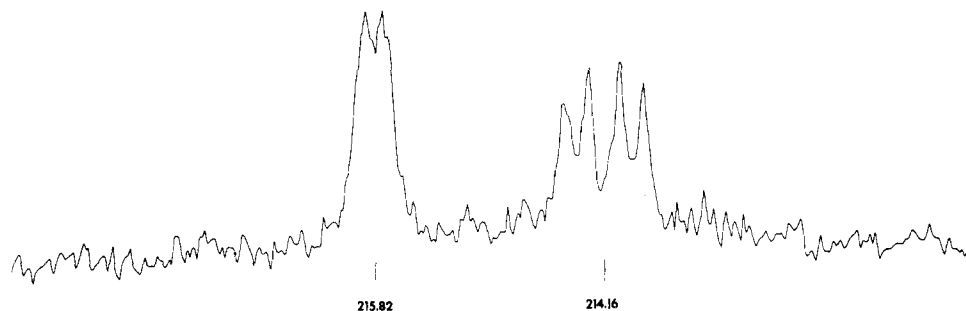


Figure 4. The 67.88-MHz ^{13}C spectrum (carbonyl region) of $(\eta^3\text{-C}_3\text{H}_5)\text{W}(\text{CO})_2(\text{dppm})\text{I}$ (XII) at -90°C .



Figure 5. The trigonal twist rearrangement proposed for $(\eta^3\text{-C}_3\text{H}_5)\text{M}(\text{CO})_2(\text{P-P})\text{X}$ complexes.

are summarized in Table IX for the iodides. These barriers were determined by line-shape analysis of temperature-dependent ^{31}P NMR spectra.

For those complexes containing diphos, it was found that further broadening occurred in the ^1H NMR spectra below -115°C . In the low-temperature ^{13}C and ^1H NMR spectra it was observed that the phenyl carbons and protons, respectively, remain somewhat broadened even at the lowest obtainable temperatures. The process most likely to cause the broadening of resonances in those complexes containing diphos involves the $\lambda \rightleftharpoons \delta$ interconversion of the five-membered chelate ring formed upon coordination of diphos to the metal. This process has been studied for the tris chelate metal systems containing ethylenediamine as the bidentate ligand.²⁹ It was estimated that the conformational interconversion between λ and δ forms in complexes containing ethylenediamine occurred with a barrier of 5–7 kcal/mol. Caulton et al. have studied ring inversions in diphos complexes with a number of coordination geometries and have found this process to be rapid on the NMR time scale.³⁰ An alternative explanation for the increased broadening in the NMR spectra at low temperatures involves the restricted rotation about the phosphorus-carbon bonds of the arylphosphines. The barrier for phosphorus-carbon bond rotation was estimated for a series of iron trialkyl- and triarylphosphine complexes and found to be on the order of 7.6 kcal/mol.³¹ Since the values of the barriers to interconversion for the dynamic process in these systems are approximately 11 kcal/mol, this rearrangement process cannot be ascribed to either of the aforementioned processes. A mechanism fully consistent with the spectral information obtained can be described as a trigonal twist, as illustrated in Figure 5. This process involves the rotation of the triangular face formed by the halogen and the two phosphorus atoms with respect to the face formed by the allyl and two carbonyl groups.

An important feature of this type of rearrangement is the limited number of permutations of sites which are allowed. This has important consequences in terms of the chirality of the molecule.

Cahn et al.³² have set forth rules for the specification of chirality at metal centers in octahedral environments. According to these rules, the rearrangement depicted in Figure 5 illustrates a molecule interconverting between *S* and *R* configurations. Enantiomerization of the metal center results

Table IX. Approximate Rate Constants and Energy Parameters

compd	$t, ^\circ\text{C}^a$	k, s^{-1}	$\Delta G^\ddagger, \text{kcal/mol}$
$(\eta^3\text{-C}_3\text{H}_5)\text{Mo}(\text{CO})_2(\text{diphos})\text{I}$	-47	280	10.6
$(\eta^3\text{-C}_3\text{H}_5)\text{Mo}(\text{CO})_2(\text{dppe})\text{I}$	-43	1290	10.0
$(\eta^3\text{-C}_3\text{H}_5)\text{Mo}(\text{CO})_2(\text{dppm})\text{I}$	-27	480	11.2
$(\eta^3\text{-C}_3\text{H}_5)\text{W}(\text{CO})_2(\text{diphos})\text{I}$	-33	480	11.0
$(\eta^3\text{-C}_7\text{H}_5)\text{W}(\text{CO})_2(\text{dppe})\text{I}$	-38	500	10.7
$(\eta^3\text{-C}_3\text{H}_5)\text{W}(\text{dppm})\text{I}$	-1	1250	11.9
$(\eta^3\text{-C}_3\text{H}_5)\text{Mo}(\text{CO})_2(\text{arphos})\text{I}$	-53	126	10.6 ^b

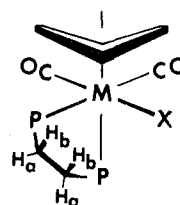
^a Temperatures were at or near coalescence. ^b Free energy barrier for major isomer \rightarrow minor isomer. Ratio = 63:37.

Table X. Relative Shifts of Protons of $(\eta^3\text{-C}_3\text{H}_5)\text{Mo}(\text{CO})_2(\text{diphos})\text{NCO}$ with Addition of $\text{Eu}(\text{thd-}d_{10})_3^a$

assignment ^b	shift ^c before addition	shift after addition	shift
H _a	2.20	3.19	0.98
H _b	2.73	4.76	2.03
H _c	3.49	5.16	1.67
H _d	1.81	2.68	0.87
H _e	3.49	4.62	1.13

^a thd- d_{10} = deuterated 2,2,6,6-tetramethyl-3,5-heptanedionate. ^b H_a and H_b are the methylene protons of the diphos. H_c is the central proton and H_d and H_e are the anti and syn protons, respectively, of the allyl ligand. ^c Shifts are in parts per million downfield from Me_4Si .

from this trigonal twist process. Similarly, enantiomerization occurs in the twist rearrangements of tris chelate metal complexes such as the Ray-Dutt or Bailar twist mechanisms.^{33,34} The trigonal twist process is consistent with the observations that in the averaged ^1H NMR spectra the methylene protons of diphos remain nonequivalent, the methylene protons of dpmm remain nonequivalent, and the terminal protons of the allyl display unequal coupling to phosphorus. Also, for this process the vinylic protons of the dppe ligand should be equivalent in the averaged spectrum; however, their observation in the ^1H NMR spectrum is obscured by the phenyl proton resonances. Despite the enantiomerization at the metal center, the spatial relationship of the P'-P''-X unit is maintained with the result that the same side of the chelating phosphine remains oriented toward the halogen. For the complexes containing diphos, therefore, one would expect equivalence of the protons indicated below in the averaged spectrum.



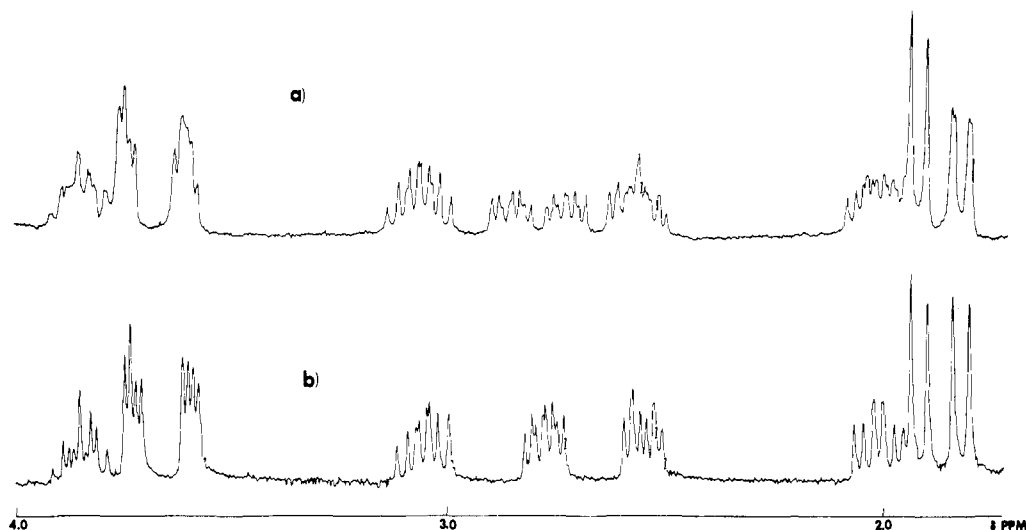


Figure 6. The 25 °C 270-MHz ^1H NMR spectrum of $(\eta^3\text{-C}_3\text{H}_5)\text{Mo}(\text{CO})_2(\text{arphos})\text{Cl}$ in CDCl_3 : (a) no decoupling; (b) ^{31}P decoupled.

The averaged ^1H NMR spectrum of $(\eta^3\text{-C}_3\text{H}_5)\text{Mo}(\text{CO})_2(\text{diphos})\text{Cl}$ shows two multiplets for the methylene protons of diphos presumably corresponding to the a and b protons (Figure 2). These resonances may be assigned on the basis of an addition of a shift reagent to the complex in which $\text{X} = \text{NCO}$. Since the magnitude of the lanthanide-induced shift, $\Delta\delta$, is proportional to the geometric factor $(1 - 3 \cos^2 \theta)/r^3$ in which r is the distance from the lanthanide to the atom in question and θ is the angle between the vector formed by r and the principal symmetry axis of the complex, one would expect to see the greatest shift for those protons closest to the binding site.³⁵⁻³⁷ Throughout the rearrangement process the b protons would be expected to remain in the closest proximity to the NCO-lanthanide binding site and therefore experience a larger shift than the a protons. The results shown in Table X indicate that the multiplet originally at 2.73 ppm in the averaged case has experienced a significantly larger lanthanide-induced shift than the multiplet at 2.20 ppm and thus the 2.73-ppm resonance can be assigned as the b protons.

The retention of the spatial relationships within the X-P'-P'' unit implies that the twist process will interconvert certain pairs of isomers in the arphos derivatives but will not invert the chirality of the As-P-X unit. In tetrahedral structures the specification of the chirality of one face is sufficient to describe completely the configuration about the center. In sufficiently complex octahedral molecules the chirality rules may not apply; nonetheless, the sense of the chirality about each of the faces can still be specified. We will consider the sense of chirality of a face to be determined by the priorities of the ligands on the triangular face, holding the metal remote (i.e., away from the viewer).³⁸ If As replaces P'' in Figure 5 an (R') -XAsP face will be retained throughout the twist process, whereas (R') -X(allyl)CO is destroyed and a new (S') -X(allyl)CO is formed. Thus, the isomerization observed for the arphos derivative might be described as an epimerization. Since the allyl-metal-dicarbonyl fragment is prochiral and the As-P-X unit should retain its chirality, the carbonyl and termini of the allyl should be diastereotopic. Thus one observes that the terminal protons of the allyl are nonequivalent in the averaged spectrum of the arphos derivative, XIII (cf. Figure 6). Separate resonances for the terminal carbons of the allyl as well as the carbonyl carbons are seen in the averaged ^{13}C NMR spectrum.

The relationship of the carbonyl groups to the allyl moiety is constant, as unequal coupling of the carbonyl carbon nuclei to the phosphorus nuclei is seen in the low-temperature carbon spectra (see Figure 5). This implies that the face formed by the

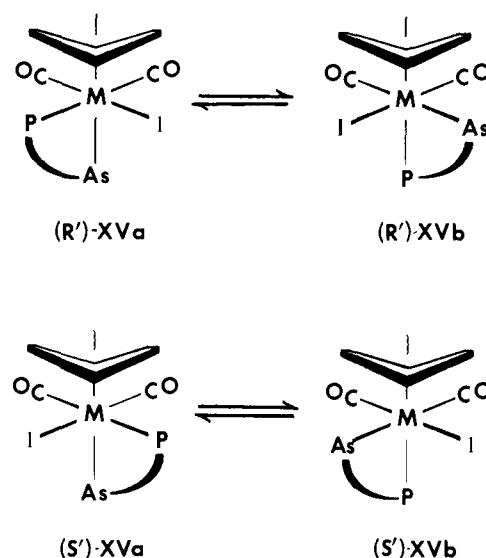


Figure 7. Allowed interconversion pathways in $(\eta^3\text{-C}_3\text{H}_5)\text{Mo}(\text{CO})_2(\text{arphos})\text{I}$.

carbonyl and the allyl group appears fixed with respect to the motion of the face formed by the halogen and two phosphorus atoms. Since diastereotopic carbonyl carbons are observed, the rearrangement retains the chirality of the (R') -(allyl)(CO)-(C'O) face.

Two enantiomeric pairs (R') -XVa, (S') -XVa and (R') -XVb, (S') -XVb are found with the arphos complex. The twist rearrangement only allows the interconversion of (R') -XVa with (R') -XVb and (S') -XVa with (S') -XVb. Therefore, if an optically active form were resolved it could not racemize by this route (cf. Figure 7). Furthermore, it is clear from the low-temperature NMR spectra that there is a significant difference in thermodynamic stability of XVa and XVb. In order to determine which isomer is more stable, the assignments must be made for the ^{13}C and ^{31}P resonances shown in Figure 8.

The $(\eta^3\text{-C}_3\text{H}_5)\text{Mo}(\text{CO})_2(\text{P-P})\text{I}$ complexes with bisphosphines show two carbonyl carbon resonances unequally coupled to phosphorus in the low-temperature spectra. It was found that in each case the carbonyl carbon exhibiting both cis and trans ^{31}P - ^{13}C splitting was shifted about 6 ppm to higher field than the carbonyl carbon with only cis splitting by phosphorus. Thus, the ^{13}C resonance of the carbonyl trans to phosphorus will generally be expected to be upfield of the other carbonyl.

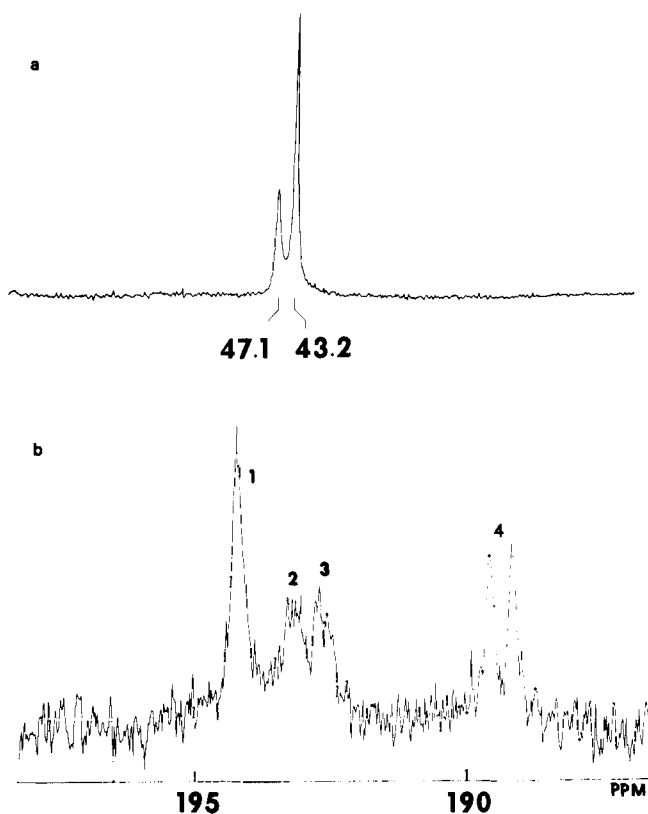


Figure 8. Low-temperature NMR spectra of $(\eta^3\text{-C}_3\text{H}_5)\text{Mo}(\text{CO})_2(\text{arphos})\text{I}$ in methylene chloride- d_2 : (a) $^{31}\text{P}\{^1\text{H}\}$ at 36.44 MHz and -53°C ; (b) $^{13}\text{C}\{^1\text{H}\}$ at 67.88 MHz and -90°C .

A distinction between the two isomers of the arphos complex, XV, can be made based upon the magnitude of the $^{31}\text{P}\text{-}^{13}\text{C}$ splittings, as well as the positions of the carbonyl ^{13}C resonances. The low-temperature carbon spectrum shows four sets of resonances with the first, second, and third positioned 6–9 ppm downfield from the fourth. The intensities of resonances 1 and 4 are comparable and greater than those of resonances 2 and 3. Based upon the trans $^{31}\text{P}\text{-}^{13}\text{C}$ coupling of 29 Hz to resonance 4, as well as its position 6 ppm above the other resonances, resonance 4 can be unambiguously assigned to the carbonyl trans to phosphorus in XVa. Resonances 2 and 3 are, therefore, consistent with carbonyls cis to phosphorus on the basis of coupling and chemical shift. Consequently, considering the relative intensities of the resonances, XVa must be the preferred isomer.

The preference for XVa is more clearly seen in the ^{31}P NMR spectrum at -53°C . The phosphorus resonance of greater intensity at -43.23 ppm can be inferred to be isomer XVa consistent with the low-temperature ^{13}C NMR spectrum. The separation between the two phosphorus resonances was 140 Hz (at 36.5 MHz) and suggests that in bisphosphine complexes this characteristic may continue and higher field resonances in bisphosphines should be assigned to the equatorial phosphorus.

A summary of the low-temperature ^{31}P data for the iodides is presented in Table XI. In the tungsten complexes the lower field resonances showed greater splittings from $^{183}\text{W}\text{-}^{31}\text{P}$ coupling. In $(\text{R}_3\text{P})_2\text{W}(\text{CO})_4$ complexes the couplings were ~ 40 Hz larger for trans than cis isomers.³⁹ This may be construed to imply that couplings should be lower when CO is trans to phosphorus. Hence, the higher field resonance in the allyl bisphosphine complexes should be assigned to an equatorial phosphorus on the basis of tungsten-phosphorus coupling in agreement with the correlation from the arphos derivative. Other apparent correlations are that increased axial-equatorial

Table XI. Separation of Phosphorus Frequencies in Low-Temperature ^{31}P NMR Spectra

compd	$\delta,^a$ Hz	$ J(\text{P-P}) $	temp, $^\circ\text{C}$
$(\eta^3\text{-C}_3\text{H}_5)\text{Mo}(\text{CO})_2(\text{arphos})\text{I}$	142		-53
$(\eta^3\text{-C}_3\text{H}_5)\text{Mo}(\text{CO})_2(\text{diphos})\text{I}$	68	<25	-57
$(\eta^3\text{-C}_3\text{H}_5)\text{W}(\text{CO})_2(\text{diphos})\text{I}^b$	98	<18	-63
$(\eta^3\text{-C}_3\text{H}_5)\text{Mo}(\text{CO})_2(\text{dppe})\text{I}$	269	<20	-63
$(\eta^3\text{-C}_3\text{H}_5)\text{W}(\text{CO})_2(\text{dppe})\text{I}^c$	557	19.5	-53
$(\eta^3\text{-C}_3\text{H}_5)\text{Mo}(\text{CO})_2(\text{dppm})\text{I}$	508	<15	-47
$(\eta^3\text{-C}_3\text{H}_5)\text{W}(\text{CO})_2(\text{dppm})\text{I}$	796	14.6	-41

^a Separation at 36.4 MHz. ^b $J(\text{W-P}) = 234$ and 177 Hz for low- and high-field resonance, respectively. ^c $J(\text{W-P}) = 216$ and 175 Hz for low- and high-field resonance, respectively. ^d $J(\text{W-P}) = 193$ and 153 Hz for low- and high-field resonance, respectively.

^{31}P shift separations are associated with tungsten compounds compared with molybdenum compounds or small bite angle chelates.

An ability to vary the barriers over a range of 6 kcal/mol can be anticipated by selection of appropriate ligands. The chlorides rearrange significantly faster than the iodides because limiting low-temperature spectra are not reached at -100°C for the chloride complexes. Reference to Table IX also indicates that bite angles also affect the rates and that dppm increases the barrier most effectively. The data indicate that all of the complexes rearrange by the twist mechanism about a single axis. This process interconverts certain pairs of isomers while retaining particular elements of chirality. It does not appear that rearrangement about other axes occurs at a significant rate; hence, when complexes of this type rearrange a pathway for racemization may not necessarily be accessible. Therefore, if a single stereomer were isolated it may epimerize but it would not rapidly racemize.

Experimental Section

General Methods. All reactions were performed under an inert nitrogen atmosphere. Tetrahydrofuran (THF) was dried over sodium and distilled from sodium benzophenone ketyl under nitrogen just prior to use. Acetonitrile was dried by refluxing with CaH_2 and distilling from CaH_2 under nitrogen. The bidentate ligands diphos, $(\text{C}_6\text{H}_5)_2\text{PCH}_2\text{CH}_2\text{P}(\text{C}_6\text{H}_5)_2$, dppe, $(\text{C}_6\text{H}_5)_2\text{PCHCHP}(\text{C}_6\text{H}_5)_2$, dppm, $(\text{C}_6\text{H}_5)_2\text{PCH}_2\text{P}(\text{C}_6\text{H}_5)_2$, and arphos, $(\text{C}_6\text{H}_5)_2\text{P}(\text{C}_6\text{H}_5)_2$, were purchased from Strem Chemicals, Inc., Danvers, Mass., and Orgmet, Inc., East Hempstead, N.H. Silica gel (Mallinckrodt SilicAR CC-7) adsorbent was employed for chromatographic procedures. ^1H NMR spectra were recorded using HA-100 and Bruker HX270 spectrometers equipped with variable-temperature accessories. The ^{13}C NMR spectra were obtained at 67.88 MHz utilizing the Bruker HX270 spectrometer. A CFT-20 and a Bruker HX90 spectrometer equipped with variable-temperature phosphorus probes were used to acquire ^{31}P NMR spectra at 32.19 and 36.5 MHz, respectively. Infrared spectra were taken on a Perkin-Elmer 421 spectrometer calibrated with gaseous DCl. Chemical analyses were performed by Baron Consulting Laboratories, Orange, Conn. Melting points in the range of $171\text{--}211^\circ\text{C}$ were obtained under a nitrogen atmosphere and are uncorrected. Analyses, melting points, and infrared data are reported in the supplementary material (Tables XIII and XIV).

Synthesis of η^3 -Allyl Molybdenum Bisphosphine Complexes. Complexes of the general formula $(\eta^3\text{-C}_3\text{H}_5)\text{Mo}(\text{CO})_2(\text{bisphosphine})\text{X}$ where $\text{X} = \text{Cl}$ or I were synthesized from the known bis-acetonitrile precursors $(\eta^3\text{-C}_3\text{H}_5)\text{Mo}(\text{CO})_2(\text{CH}_3\text{CN})_2\text{X}$. The diphos derivatives have been previously reported. A typical reaction involved the addition of a bisphosphine to an equimolar amount of $(\eta^3\text{-C}_3\text{H}_5)\text{Mo}(\text{CO})_2(\text{CH}_3\text{CN})_2\text{X}$ in THF at room temperature. The mixture was allowed to stir for 0.5 h, after which the solvent was removed. A minimal amount of methylene chloride was used to bring the crude product into solution which was then loaded onto a column prepared with silica gel. The product was eluted with methylene chloride and gave yields from 85 to 90%. Crystallization of the molybdenum bisphosphine complexes was performed using methylene chloride/hexane mixtures. The physical properties of the π -allyl

molybdenum bisphosphine complexes are reported in Table XIII.

Synthesis of $(\eta^3\text{-C}_3\text{H}_5)\text{Mo}(\text{CO})_2(\text{diphos})\text{NCO}$ (XVI). The isocyanate derivative was synthesized by addition of silver isocyanate to a methylene chloride solution of $(\eta^3\text{-C}_3\text{H}_5)\text{Mo}(\text{CO})_2(\text{diphos})\text{Cl}$ at room temperature. The mixture was allowed to stir overnight and subsequent filtration through Celite removed AgCl and the other silver salts. The filtrate was concentrated and loaded onto a column prepared with silica gel. The product eluted with methylene chloride and was recrystallized from methylene chloride/hexane affording the complex XVI in 95% yield. The infrared spectrum of XVI shows $\nu(\text{NCO})$ 2218 cm^{-1} and $\nu(\text{CO})$ 1940 and 1848 cm^{-1} (CH_2Cl_2) with the position of the former mode establishing that the isocyanate ligand is N bonded to the metal atom.

Synthesis of η^3 -Allyl Tungsten Bisphosphine Complexes. Three general methods were employed for preparation of the tungsten bisacetonitrile precursors of the general formula $(\eta^3\text{-C}_3\text{H}_5)\text{W}(\text{CO})_2(\text{CH}_3\text{CN})_2\text{X}$ where X = Cl or I.

Method I. Tungsten hexacarbonyl and acetonitrile were allowed to reflux for approximately 40 h. Aliquots of the bisacetonitrile species $(\text{CH}_3\text{CN})_2\text{W}(\text{CO})_4$ formed at this point were added to 300 mL of acetonitrile in a jacketed Pyrex photolysis tube through which cold water was circulated. The appropriate allyl halide was added to the vessel and an ultraviolet sunlamp used for the irradiation was placed about 3 cm from the outside of the vessel. The reaction was monitored by infrared spectroscopy and presumed complete once the absorptions corresponding to $(\text{CH}_3\text{CN})_2\text{W}(\text{CO})_4$ were replaced by those of the desired product, $(\eta^3\text{-C}_3\text{H}_5)\text{W}(\text{CO})_2(\text{CH}_3\text{CN})_2\text{X}$. The acetonitrile was removed in vacuo, producing the compounds $(\eta^3\text{-C}_3\text{H}_5)\text{W}(\text{CO})_2(\text{CH}_3\text{CN})_2\text{X}$ in 50–60% yield.

Method II. Tungsten hexacarbonyl and acetonitrile were allowed to reflux for approximately 2 weeks. It was only after this lengthy interval that the trisacetonitrile tungsten tricarbonyl was formed in reasonable quantities. The acetonitrile was removed in vacuo affording $(\text{CH}_3\text{CN})_3\text{W}(\text{CO})_3$ as a light brown powder: $\nu(\text{CO})$ 1910, 1790 cm^{-1} in CH_3CN (lit. 1913, 1790 cm^{-1} in CH_3CN). A portion of the trisacetonitrile complex was then dissolved in THF, the appropriate allylic halide added, and the solution allowed to stir at 60 °C for 1 h. The color changed from yellow-brown to orange and finally to orange-red as the reaction neared completion. Evaporation of the THF solvent produced $(\eta^3\text{-C}_3\text{H}_5)\text{W}(\text{CO})_2(\text{CH}_3\text{CN})_2\text{X}$ in yields of 80–95%.

Method III. The $(\text{CH}_3\text{CN})_3\text{W}(\text{CO})_3$ could also be obtained photolytically using ultraviolet radiation supplied by a 450-W mercury arc lamp. In a typical preparation 1.0 g of $\text{W}(\text{CO})_6$ was added to a well containing 300 mL of acetonitrile. A water-jacketed quartz tube containing the lamp was placed inside the well. The $\text{W}(\text{CO})_6$ /acetonitrile solution was then irradiated for 30 h. The trisacetonitrile tungsten tricarbonyl compound thus formed was used for further reaction with the chosen allyl halide. The overall yield of $(\eta^3\text{-C}_3\text{H}_5)\text{W}(\text{CO})_2(\text{CH}_3\text{CN})_2\text{X}$ was 60%.

Once $(\eta^3\text{-C}_3\text{H}_5)\text{W}(\text{CO})_2(\text{CH}_3\text{CN})_2\text{X}$ had been formed, an equimolar amount of bisphosphine was added and the mixture was allowed to stir at 60 °C for 1 h. The tungsten-bisphosphine complexes thus formed were purified in a manner identical with that of the molybdenum analogues. Yields of the tungsten-bisphosphine complexes ranged from 80 to 95%.

Collection and Reduction of the X-ray Diffraction Data. Crystals of $(\eta^3\text{-C}_3\text{H}_5)\text{Mo}(\text{CO})_2(\text{diphos})\text{Cl}$ (I) suitable for crystallographic examination were obtained by crystallization from methylene chloride/hexanes (3/1) by cooling to –20 °C. An orange, crystalline plate with dimensions 0.3 × 0.12 × 0.055 mm was chosen and mounted in a thin-walled glass capillary. Preliminary precession photographs indicated monoclinic symmetry. Verification of the symmetry was made by the centering and processing of 15 randomly collected reflections on an Enraf-Nonius CAD-4 automatic diffractometer. Inspection of the data revealed the systematic absences $0k0$, $k = 2n + 1$, and $h0l$, $h + l = 2n + 1$, uniquely identifying the space group as $P2_1/n$. The centering and least-squares refinement of 12 high-angle reflection ($2\theta > 20^\circ$) utilizing a Picker FACS-I automatic diffractometer gave accurate unit cell parameters. The cell parameters along with crystal data are reported in Table XII. After the crystal faces $\{010\}$, $\{10\bar{1}\}$, and $\{101\}$ were identified, the crystal was mounted on a Picker FACS-I automatic diffractometer with its b axis coincident with the diffractometer ϕ axis.

Solution and Refinement of the Structure. The structure was solved by heavy atom methods. A three-dimensional Patterson synthesis provided the coordinates of the molybdenum atom. Two cycles of

Table XII. Experimental X-ray Diffraction Data for $(\eta^3\text{-C}_3\text{H}_5)\text{Mo}(\text{CO})_2\text{Cl}((\text{C}_6\text{H}_5)_2\text{P}(\text{CH}_2)_2\text{P}(\text{C}_6\text{H}_5)_2)$ (I)

A. Crystal Data	
space group	$P2_1/n$, C_{2h}^5
temp	20 °C
cell parameters	$a = 11.422$ (6) Å $b = 18.004$ (12) Å $c = 14.504$ (8) Å $\beta = 106.54$ (3)°
Z	4
ρ_{calcd}	1.456 g cm^{-3}
ρ_{obsd}	1.460 g cm^{-3} (flotation)
μ	6.84
B. Intensity Measurement Data	
radiation	Mo $K\alpha$ $\lambda = 0.71609$ Å
monochromator	graphite
takeoff angle	2.2°
detector aperture	4 × 4 mm
reflections measured	+ h , + k , + l
2θ data range	0–55°
scan type	θ – 2θ
2θ scan speed	2.0° min^{-1}
2θ scan width	$K\alpha_1 - 0.75^\circ$ to $K\alpha_2 + 0.75^\circ$
backgrounds	10 s (stationary at each end of scan)
no. data	2131
data used [$F^2 > 3.0\sigma(F^2)$]	1878
R factor	0.04

full-matrix least-squares refinement with an isotropic temperature factor produced the unweighted and weighted residuals

$$R = (\sum |F_o| - |F_c|) / \sum |F_o|$$

$$R_w = (\sum w_i (|F_o| - |F_c|)^2 / \sum w_i F_o^2)^{1/2}$$

of 0.39 and 0.51, respectively. The weights, w_i , were based upon the relation $1/\sigma(F_o)^2$, and the function minimized in the least squares was $\sum w_i (|F_o| - |F_c|)^2$. Neutral atom scattering factors were calculated by the method of Cromer and Waber. The remaining nonhydrogen atoms were found by a series of difference Fourier syntheses. Anomalous dispersion corrections $\Delta f'$ and $\Delta f''$ were made for the molybdenum, phosphorus, and chlorine atoms. Three intense reflections were monitored approximately once every 150 reflections and showed only random $\pm 3\%$ fluctuations in intensity during the course of the data collection. No decay or absorption correction was applied.

The hydrogen atoms were calculated in stereochemically credible positions at distances of 0.95 Å assuming tetrahedral symmetry for the methylene carbons in the chelate ligand and sp^2 (trigonal) symmetry for the allyl group. The phenyl rings were assumed to be planar and to possess sixfold symmetry. Hydrogen atom contributions were added to structure factor calculations but these positions were not refined.

Refinement converged to produce the final residuals, $R = 0.060$ and $R_w = 0.057$. The largest shift vs. error value given on the final cycle of refinement was 0.48 with most values under 0.20. The error in an observation of unit weight, $[\sum w_i (|F_o| - |F_c|)^2 / (\text{NO} - \text{NV})]^{1/2}$, was 1.17. The last structure factor calculation confirmed that the values for the rejected reflections were all acceptably low. A final difference Fourier synthesis was featureless. The largest peaks were 0.60 and 0.50 $e/\text{Å}^3$ and were in the vicinity of the molybdenum atom.

The rates and free energies of activation were computed using a Kubo-Sack line shape analysis program^{3,40,41} modified for use on a PDP 11/10. The AB cases for the ³¹P spectra were calculated using the probabilities for exchange between resonances 1 and 3, as well as 2 and 4, appropriate to the relative intensities.^{42,43} In situations where the coupling was not resolved at low temperature, it was estimated at 20 Hz. Because the chemical shifts are large a variation of splitting between 10 and 20 Hz has an insignificant effect upon the ΔG^\ddagger obtained.

Acknowledgment. This research was supported by National Science Foundation Grant CHE77-14943. The services of the 270-MHz NMR were made available by a grant from the

Biotechnology Resources Program of the National Institutes of Health (RR-798). The 36.44-MHz ^{31}P spectra were obtained through the courtesy of Professor Ian Armitage.

Supplementary Material Available: Infrared data (Table XIII); melting points and analyses (Table XIV); observed and calculated structure factors (Table XV); thermal parameters (Table XVI); nonhydrogen intermolecular contacts less than 3.75 Å (Table XVII); view of the unit cell showing four molecules (Figure 9) (17 pages). Ordering information is given on any current masthead page.

References and Notes

- (1) E. L. Muetterties, *Inorg. Chem.*, **4**, 769 (1965).
- (2) E. L. Muetterties, *Acc. Chem. Res.*, **3**, 266 (1970).
- (3) L. M. Jackman and F. A. Cotton, Ed., "Dynamic Nuclear Magnetic Resonance Spectroscopy", Academic Press, New York, N.Y., 1975.
- (4) F. A. Cotton, *Acc. Chem. Res.*, **1**, 257 (1968).
- (5) The most extensive work on stereochemically nonrigid octahedral complexes which does not involve chelates has been undertaken by W. A. G. Graham: L. Vancea, M. J. Bennett, D. E. Jones, R. A. Smith, and W. A. G. Graham, *Inorg. Chem.*, **16**, 897 (1977); R. K. Pomeroy, L. Vancea, H. P. Calhoun, and W. A. G. Graham, *J. Am. Chem. Soc.*, **98**, 1407 (1976); R. K. Pomeroy, L. Vancea, H. P. Calhoun, and W. A. G. Graham, *Inorg. Chem.*, **16**, 1508 (1977).
- (6) L. H. Pignolet and G. N. LaMar in "NMR of Paramagnetic Molecules Principles and Applications", G. N. LaMar, W. Dew. Horrocks, Jr., and R. H. Holm, Ed., Academic Press, New York, N.Y., 1973, p 333.
- (7) R. H. Holm in "Dynamic Nuclear Magnetic Resonance Spectroscopy", L. M. Jackman and F. A. Cotton, Ed., Academic Press, New York, N.Y., 1975, p 317.
- (8) J. D. Morrison, W. F. Masler, and K. Neuberg, *Adv. Catal.*, **25**, 81 (1976).
- (9) L. Marko and B. Heil, *Catal. Rev.*, **8**, 269 (1973).
- (10) M. D. Fryzuk and B. Bosnich, *J. Am. Chem. Soc.*, **99**, 6262 (1977).
- (11) J. W. Faller and A. M. Rosan, *Ann. N.Y. Acad. Sci.*, **295**, 186 (1977).
- (12) The abbreviation "P-P" is used to denote a bidentate ligand such as dppp = *cis*-bis(diphenylphosphino)ethylene; diphos = bis(diphenylphosphino)ethane; dppm = bis(diphenylphosphino)methane; arphos = 1-(diphenylphosphino)-2-(diphenylarsino)ethane; diars = bis(diphenylarsino)ethane.
- (13) A. J. Graham and R. H. Fenn, *J. Organomet. Chem.*, **17**, 405 (1969).
- (14) R. H. Fenn and A. J. Graham, *J. Organomet. Chem.*, **37**, 137 (1972).
- (15) A. J. Graham and R. H. Fenn, *J. Organomet. Chem.*, **25**, 173 (1970).
- (16) F. Dawans, J. Dewally, J. Meunier-Piret, and P. Piret, *J. Organomet. Chem.*, **76**, 53 (1974).
- (17) J. W. Faller, D. A. Haitko, R. D. Adams, and D. F. Chodos, *J. Am. Chem. Soc.*, **99**, 1654 (1977).
- (18) B. J. Brisdon and A. A. Woolf, *J. Chem. Soc., Dalton Trans.*, 291 (1978).
- (19) B. J. Brisdon and G. F. Griffin, *J. Chem. Soc., Dalton Trans.*, 1999 (1975).
- (20) B. J. Brisdon, *J. Organomet. Chem.*, **125**, 225 (1977). (The results for these molybdenum-bisphosphine complexes were interpreted incorrectly as arising from structure A.)
- (21) U. Franke and E. Weiss, *J. Organomet. Chem.*, **121**, 355 (1976).
- (22) U. Franke and E. Weiss, *J. Organomet. Chem.*, **153**, 39 (1978).
- (23) M. A. Bush, A. D. V. Hardy, Lj. Manojlovic-Muir, and G. A. Sim, *J. Chem. Soc. A*, 1003 (1971).
- (24) M. G. B. Drew, *J. Chem. Soc., Dalton Trans.*, 1329 (1972).
- (25) F. W. B. Einstein and J. S. Field, *J. Chem. Soc., Dalton Trans.*, 1628 (1975).
- (26) S. Chaiwasie and R. H. Fenn, *Acta Crystallogr., Sect. B*, **24**, 525 (1968).
- (27) F. A. Cotton, B. A. Frenz, and A. G. Stanislawski, *Inorg. Chim. Acta*, **7**, 503 (1973).
- (28) P. S. Braterman, D. W. Milne, E. W. Randall, and E. Rosenberg, *J. Chem. Soc., Dalton Trans.*, 1207 (1973).
- (29) J. K. Beattie, *Acc. Chem. Res.*, **4**, 253 (1971).
- (30) P. R. Hoffman, J. S. Miller, C. B. Ungermann, and K. G. Caulton, *J. Am. Chem. Soc.*, **95**, 7902 (1973).
- (31) J. W. Faller and B. V. Johnson, *J. Organomet. Chem.*, **96**, 99 (1975).
- (32) R. S. Cahn, C. Ingold, and V. Prelog, *Angew. Chem., Int. Ed. Engl.*, **5**, 385 (1966).
- (33) P. Ray and N. K. Dutt, *J. Indian Chem. Soc.*, **20**, 81 (1943).
- (34) J. C. Bailar, *J. Inorg. Nucl. Chem.*, **8**, 165 (1958).
- (35) H. M. McConnell and R. E. Robertson, *J. Chem. Phys.*, **29**, 1361 (1958).
- (36) R. J. Kurland and B. R. McGarvey, *J. Magn. Reson.*, **2**, 286 (1970).
- (37) W. Dew. Horrocks, Jr., *Inorg. Chem.*, **9**, 690 (1970).
- (38) Rules for defining chirality of octahedral complexes break down in these systems. We have defined the new terms R' and S' , which describe the chirality of a triangular face with the metal held remote from the viewer. Priority rules are the same as previously defined, with the exception that the presence of a chelate is not assumed to raise the priority. Thus in the case of the arphos iodide complex, the priority order is $I > As > P$.
- (39) S. O. Grim and D. A. Wheatland, *Inorg. Nucl. Chem. Lett.*, **4**, 187 (1968).
- (40) M. Saunders, *Tetrahedron Lett.*, 1699 (1963).
- (41) R. A. Sack, *Mol. Phys.*, **1**, 163 (1958).
- (42) C. S. Johnson, Jr., *J. Magn. Reson.*, **1**, 98 (1969).
- (43) R. M. Lyndon-Bell, *Prog. Nucl. Magn. Reson. Spectrosc.*, **2**, 163 (1967).